

Efficient Fourier representations of families of Gaussian processes

Philip Greengard*

October 18, 2022

Abstract

We introduce a class of algorithms for constructing Fourier representations of Gaussian processes in 1 dimension that are valid over ranges of hyperparameter values. The scaling and frequencies of the Fourier basis functions are evaluated numerically via generalized quadratures. The representations introduced allow for $O(N + m^3)$ inference via the non-uniform FFT where N is the number of data points and m is the number of basis functions. Numerical results are provided for Matérn kernels with $\nu \in [3/2, 7/2]$ and $\rho \in [0.1, 0.5]$. The algorithms of this paper generalize mathematically to higher dimensions, though they suffer from the standard curse of dimensionality.

1 Introduction

Gaussian process (GP) regression has become ubiquitous as a statistical tool in many applied sciences including astrophysics, environmental sciences, molecular dynamics, financial economics, and social sciences [2, 4, 7, 12, 13, 14, 24, 35].

In most Gaussian process regression problems a user has observed data $\{(x_i, y_i)\}$ where x_1, \dots, x_N are independent variables that belong to some set $D \subseteq \mathbb{R}^d$ and $y_i \in \mathbb{R}$ are dependent variables. The observed data y_1, \dots, y_N are assumed to be observations of the form

$$y_i = f(x_i) + \epsilon_i \quad (1)$$

where ϵ_i is iid Gaussian noise, and $f : D \rightarrow \mathbb{R}$ is given a Gaussian process prior $f(x) \sim \mathcal{GP}(\mu(x), k(x, x'))$ where μ is a user-specified mean function and k is a covariance function [31].

The primary computational limitation of GP regression as a practical tool is the prohibitive cost of the matrix inversion that appears in the likelihood function of a Gaussian process

$$p(\mathbf{y}) \propto \frac{1}{|\mathbf{K} + \sigma^2 \mathbf{I}|^{1/2}} \exp^{-\frac{1}{2} \mathbf{y}^T (\mathbf{K} + \sigma^2 \mathbf{I})^{-1} \mathbf{y}} \quad (2)$$

*Department of Statistics, Columbia University, pg2118@columbia.edu. Research supported by the Alfred P. Sloan Foundation.

where \mathbf{K} is the $N \times N$ matrix such that $\mathbf{K}_{i,j} = k(x_i, x_j)$ and σ^2 is the variance of the independent and identically distributed (iid) observation noise. For a general symmetric matrix, direct inversion of the covariance matrix \mathbf{K} in (2) requires $O(N^3)$ operations, which for many modern problems is far too costly. A large body of literature has emerged over the last couple of decades on efficient schemes for evaluating that quadratic form when N is large (i.e. greater than around 10,000). Often, these computational methods rely on taking advantage of the particular structure of covariance matrices [1, 12, 26], approximating the covariance matrix with a low rank matrix (reduced-rank methods) [17, 28, 34], spectral methods [18, 21, 29], or many more strategies.

In this paper we introduce numerical algorithms for representing a zero-mean Gaussian process f with a translation invariant covariance kernel k as a random expansion of the form

$$f(x) \sim \gamma_1 \alpha_1 \cos(\xi_1 x) + \beta_1 \gamma_1 \sin(\xi_1 x) + \dots + \alpha_m \gamma_m \cos(\xi_m x) + \beta_m \gamma_m \sin(\xi_m x) \quad (3)$$

where for $i = 1, \dots, m$ the frequencies $\xi_i \in \mathbb{R}$ are fixed, and α_i and β_i are the iid Gaussians

$$\alpha_i, \beta_i \sim \mathcal{N}(0, 1). \quad (4)$$

The coefficients γ_i of (3) are defined by

$$\gamma_i = \sqrt{2w_i \hat{k}(\xi_i)} \quad (5)$$

where \hat{k} denotes the Fourier transform of the covariance kernel and $w_i > 0$. The numerical work in constructing expansion (3) involves finding the frequencies ξ_i and the weights w_i such that expansion (3) has an effective covariance kernel that approximates the desired kernel (or family of kernels) to high accuracy. We provide numerical results for constructing an expansion of the form (3) that is valid for all Matérn kernels with $\rho \in [0.1, 0.5]$, and $\nu \in [3/2, 7/2]$.

There are several advantages to using expansion (3) as a representation of a family of GPs. One computational benefit stems from the so-called weight-space approach to Gaussian process regression (see e.g. [31], [17], [11]) in which the posterior density is defined over the coefficients of basis function expansion – in this paper expansion (3). Specifically, given data $\{(x_i, y_i)\}$ and a covariance kernel k , weight-space Gaussian process regression is the L^2 -regularized linear regression

$$\begin{aligned} \mathbf{y} &\sim \mathbf{X}\boldsymbol{\beta} + \boldsymbol{\epsilon} \\ \boldsymbol{\epsilon} &\sim \mathcal{N}(0, \sigma^2 \mathbf{I}) \\ \boldsymbol{\beta} &\sim \mathcal{N}(0, \mathbf{I}) \end{aligned} \quad (6)$$

where $\boldsymbol{\beta} \in \mathbb{R}^{2m}$ is the vector of coefficients and \mathbf{X} is the $N \times 2m$ matrix

$$\mathbf{X} = \begin{bmatrix} \gamma_1 \cos(\xi_1 x_1) & \dots & \gamma_m \cos(\xi_m x_1) & \gamma_1 \sin(\xi_1 x_1) & \dots & \gamma_m \sin(\xi_m x_1) \\ \gamma_1 \cos(\xi_1 x_2) & \dots & \gamma_m \cos(\xi_m x_2) & \gamma_1 \sin(\xi_1 x_2) & \dots & \gamma_m \sin(\xi_m x_2) \\ \vdots & & \vdots & \vdots & & \vdots \\ \gamma_1 \cos(\xi_1 x_N) & \dots & \gamma_m \cos(\xi_m x_N) & \gamma_1 \sin(\xi_1 x_N) & \dots & \gamma_m \sin(\xi_m x_N) \end{bmatrix}.$$

The posterior density corresponding to (6) is defined over $2m$ dimensions (components of β) and the conditional (or posterior) mean function is given by

$$\sum_{i=1}^m \bar{\beta}_{1,i} \gamma_i \cos(\xi_i x) + \bar{\beta}_{2,i} \gamma_i \sin(\xi_i x) \quad (7)$$

where $[\bar{\beta}_1 \bar{\beta}_2]^\top$ is the solution to the linear system of equations

$$(\mathbf{X}^\top \mathbf{X} + \sigma^2 \mathbf{I})x = \mathbf{X}^\top \mathbf{y}. \quad (8)$$

Representing a GP with Fourier expansion (3) has the advantage that GP regression via linear system (8) can be solved in $O(N + m^3)$ operations. For a general $N \times 2m$ matrix, \mathbf{X} , solving linear system (8) requires $O(Nm^2)$ operations, which can be prohibitively expensive for big data problems. However since we use Fourier expansions, the $2m \times 2m$ matrix $\mathbf{X}^\top \mathbf{X}$ can be formed in $O(N + m^2 \log m)$ operations using a non-uniform fast Fourier transform (FFT) [9, 15]. The efficient formation of $\mathbf{X}^\top \mathbf{X}$ reduces the total computational cost of solving the linear system from $O(Nm^2)$ operations to $O(N + m^3)$. In general, m is sufficiently small that m^3 operations is easily affordable on a laptop. Furthermore, for GP problems that involve fitting hyperparameters, the cost of solving linear system (8) is $O(m^3)$ operations for all hyperparameters after a precomputation of $O(N + m^2 \log m)$ operations.

The numerical work in finding ξ_i and w_i of expansion (3) reduces to constructing a quadrature rule (see, e.g. [25]) for computing the inverse Fourier transform of \hat{k} , the Fourier transform of the covariance kernel. Specifically, if k is an integrable translation-invariant covariance kernel with Fourier transform \hat{k} , then k satisfies

$$k(d) = \int_{\mathbb{R}} \hat{k}(\xi) e^{i\xi d}. \quad (9)$$

It turns out that we can construct expansion (3) by evaluating $\xi_i \in \mathbb{R}$ and $w_i \in \mathbb{R}^+$ such that $k(d)$ is well approximated by the sum

$$\sum_{j=1}^n w_j \hat{k}(\xi_j) e^{i\xi_j d} \quad (10)$$

for a family of covariance kernels where d is in some region of interest.

In this paper, we find ξ_i and w_i by using algorithms for constructing generalized Gaussian quadratures. The theory associated with generalized Gaussian quadratures was originally introduced in 1966 [20] and more recently, efficient numerical algorithms have made constructing generalized Gaussian quadratures practical in many modern problems [6, 25]. The use of such quadratures is now widespread in several environments including in computational physics for the solution of integral equations with singular kernels, and in the numerical solution of certain partial differential equations (e.g. [5, 19, 25]).

The basis function approach of this paper is similar in spirit to several popular basis function approaches including [22, 30]. In particular, the GP basis function representations of this paper are closely related to those of [17]. In [17] a Gaussian process on an interval

$[a, b]$ is approximated with a so-called Karhunen-Loève (KL) expansion, an expansion of the form

$$\alpha_1 f_1(x) + \dots + \alpha_n f_n(x) \quad (11)$$

where $\alpha_i \sim \mathcal{N}(0, 1)$ are iid and f_i are eigenfunctions of the integral operator

$$\int_a^b k(x, y) f(y) dy \quad (12)$$

where $k : [a, b] \times [a, b] \rightarrow \mathbb{R}$ is the covariance kernel. The primary advantage of KL-expansions is that for any expansion of length m , the KL-expansion is optimal in the sense that its effective covariance kernel approximates the exact covariance kernel in L^2 better than any other expansion of length m .

The methods of this paper, however, have two primary advantages over those of other basis function approaches such as [17].

- Fourier basis functions are amenable to fast algorithms for solving the linear systems of GP regression. We capitalize on this fact to obtain $O(N + m^3)$ computational complexity for GP regression.
- The Fourier expansions of this paper are valid over families of covariance kernels, whereas those of other basis function approaches require recomputing basis functions for kernels with different hyperparameter values. As a result, adaptation of hyperparameters is simplified. For all hyperparameter values in the domain of the Fourier expansion, GP regression is performed in $O(m^2)$ operations after a precomputation of $O(N + m^3)$ operations.

Another similar approach to the one of this paper can be found in [33] where the authors use a quadrature rule in Fourier domain in order to construct low-rank approximations of covariance matrices.

The remainder of this paper is structured as follows. In the following section, we introduce theoretical and numerical tools for representing GPs as Fourier expansions. In Section 3 we describe fast algorithms for GP regression. We provide the numerical results of the algorithms of this paper in Section 4. We conclude with a brief discussion of future directions of research in Section 5.

2 Spectral representation of GPs

Translation invariant (or stationary) covariance kernels are commonly used in practice and include kernel families such as Matérn, squared-exponential, rational quadratic, periodic, and many more [31]. A translation invariant kernel is a function $k(x, y) : \mathbb{R}^d \times \mathbb{R}^d \rightarrow \mathbb{R}$ that can be expressed as a function of $x - y$. In a slight abuse of notation we refer to translation invariant kernels $k(x, y)$ as functions of one variable, $k(d)$ for $d \in \mathbb{R}$.

All of the previously mentioned stationary kernels are also isotropic, that is, they are functions $k(x, y)$ that depend on $\|x - y\|$. For those kernels, $k(d) = k(-d)$, their Fourier

transforms are real-valued and symmetric. However, not all symmetric functions are valid covariance kernels. Translation invariant kernels have a particular property – k is a valid kernel if and only if its Fourier transform is non-negatively valued. This property is known as Bochner’s theorem [31].

Clearly an integrable translation-invariant kernel k can be expressed as the inverse Fourier transform

$$k(d) = \int_{-\infty}^{\infty} \hat{k}(\xi) e^{2\pi i \xi d} d\xi, \quad (13)$$

where \hat{k} denotes the Fourier transform of k . Or equivalently, since \hat{k} is even,

$$k(d) = \int_0^{\infty} 2\hat{k}(\xi) \cos(2\pi \xi d) d\xi. \quad (14)$$

A discretized version of integral (14), or an order- n quadrature rule for approximating the integral is a sum of the form

$$k(d) = \sum_{j=1}^n 2w_j \hat{k}(\xi_j) \cos(2\pi \xi_j d). \quad (15)$$

where $\xi_j > 0$ and $w_j \in \mathbb{R}$. The following theorem shows that any sum of the form (15) corresponds to a basis function representation of a Gaussian process with a covariance kernel that approximates k with the accuracy of discretization (15).

Theorem 1. *Let f be the random expansion defined by*

$$f(x) \sim \sum_{i=1}^m \alpha_i \gamma_i \cos(\xi_i x) + \beta_i \gamma_i \sin(\xi_i x) \quad (16)$$

where for all $i, j = 1, \dots, m$ the random coefficients α_i and β_j are iid and

$$\alpha_i, \beta_j \sim \mathcal{N}(0, 1) \quad (17)$$

and where γ_i are defined by

$$\gamma_i = \sqrt{2w_i \hat{k}(\xi_i)} \quad (18)$$

where \hat{k} denotes the Fourier transform of the covariance kernel k and $\xi_i, w_i > 0$. Then f is a Gaussian process with covariance kernel k' defined by the formula

$$k'(d) = \sum_{i=1}^m 2w_i \hat{k}(\xi_i) \cos(2\pi \xi_i d). \quad (19)$$

Proof. Using the independence of the Gaussian coefficients of f , clearly,

$$\begin{aligned} E[f(x)f(y)] &= \sum_{j=1}^m 2w_j \hat{k}(\xi_j) \cos(2\pi \xi_j x) \cos(2\pi \xi_j y) + \sum_{j=1}^m 2w_j \hat{k}(\xi_j) \sin(2\pi \xi_j x) \sin(2\pi \xi_j y) \\ &= \sum_{j=1}^m 2w_j \hat{k}(\xi_j) \left(\cos(2\pi \xi_j x) \cos(2\pi \xi_j y) + \sin(2\pi \xi_j x) \sin(2\pi \xi_j y) \right) \end{aligned} \quad (20)$$

Applying standard trigonometric properties to (20), we obtain

$$E[f(x)f(y)] = \sum_{j=1}^m 2w_j \hat{k}(\xi_j) \cos(2\pi\xi_j(x-y)). \quad (21)$$

□

An immediate consequence of Theorem 1 is that an m -point quadrature rule for the evaluation of the inverse Fourier transform of a covariance kernel provides a weight-space representation of that Gaussian process. Moreover the accuracy of the quadrature rule is exactly the accuracy of the effective covariance kernel. This leads to a natural tradeoff: the more terms in an expansion, the greater the accuracy of the effective covariance kernel but the less compressed the GP representation. We now describe the numerical procedure we use for constructing the quadrature rule.

2.1 Gaussian quadratures for covariance kernels

In the numerical scheme of [6] for constructing Gaussian quadratures, the user inputs functions $\phi_1, \dots, \phi_n : [a, b] \rightarrow \mathbb{R}$ for some $n > 1$ and is returned the nodes $x_1, \dots, x_m \in [a, b]$ and weights $w_1, \dots, w_m \in \mathbb{R}^+$ such that

$$\left| \int_a^b \phi_j(x) dx - \sum_{i=1}^m w_i \phi_j(x_i) \right| < \epsilon \quad (22)$$

for some user-specified $\epsilon > 0$ for all $j = 1, \dots, n$.

In this paper, we are concerned with constructing a particular class of quadrature rules. If f is a Gaussian process defined on $[a, b]$ with covariance kernel k , then we seek to approximate integrals of the form

$$\int_0^\infty 2\hat{k}(\xi) \cos(2\pi\xi t) d\xi \quad (23)$$

for all $t \in [0, b-a]$, which contains $\{|x-y| : x, y \in [a, b]\}$. We therefore use the numerical scheme in [6] to construct quadrature rules for the set of functions

$$\phi_j(\xi) = 2\hat{k}(\xi) \cos(2\pi\xi t_j) \quad (24)$$

for $j = 1, 2, \dots, n$ and $\xi \in [0, \infty)$. Since the integrals in (23) are smooth functions in t , it is sufficient to choose t_1, \dots, t_n as, for example, order- n Chebyshev nodes on $[0, b-a]$ [36], provided that n is sufficiently large. Specifically, suppose that we construct a quadrature rule with nodes $\xi_1, \dots, \xi_m > 0$ and $w_1, \dots, w_m > 0$ such that

$$\left| \int_0^\infty 2\hat{k}(\xi) \cos(2\pi\xi t_j) d\xi - \sum_{i=1}^m 2w_i \hat{k}(\xi_i) \cos(2\pi\xi_i t_j) \right| < \epsilon \quad (25)$$

for some user-specified $\epsilon > 0$ and $j = 1, \dots, n$. Then for sufficiently large n ,

$$\left| \int_0^\infty 2\hat{k}(\xi) \cos(2\pi\xi t) d\xi - \sum_{i=1}^m 2w_i \hat{k}(\xi_i) \cos(2\pi\xi_i t) \right| < \epsilon \quad (26)$$

for all $t \in [0, b - a]$.

Similarly, we can use the same strategy to discretize a family of covariance functions over ranges of hyperparameters, provided that \hat{k} is a smooth function of those hyperparameters. For example, suppose that f is a GP defined on $[-1, 1]$ with a Matérn kernel. Now consider the set of covariance kernels k_{ν_i, ρ_j} for $i, j = 1, \dots, p$ where ν_1, \dots, ν_p are the order- p Chebyshev nodes on $[3/2, 7/2]$ and ρ_1, \dots, ρ_p are the order- p Chebyshev nodes defined on $[0.1, 0.5]$. Then \hat{k} is a smooth function of ν, ρ over their domain and we can use [6] to construct quadrature rules for the family of integrals

$$\int_0^\infty 2\hat{k}_{\nu_i, \rho_j}(\xi) \cos(2\pi\xi t_\ell) d\xi \quad (27)$$

for all $i, j \in \{1, \dots, p\}$ and $\ell \in \{1, \dots, n\}$ up to some tolerance ϵ . For large enough p and n , the resulting quadrature rules satisfy

$$\left| \int_0^\infty 2\hat{k}(\xi) \cos(2\pi\xi t) d\xi - \sum_{i=1}^m 2w_i \hat{k}(\xi_i) \cos(2\pi\xi_i t) \right| < \epsilon \quad (28)$$

for all $t \in [0, 2]$, $\rho \in [0.1, 0.5]$, $\nu \in [3/2, 7/2]$.

We used the implementation of [32] for this particular computation with $p = 100$ and $n = 200$. The code took 88 seconds to run on a laptop and returned 86 nodes ξ_1, \dots, ξ_{86} and positive weights w_1, \dots, w_{86} . The results of numerical experiments using this quadrature rule are included in Section 4 and the nodes and weights are listed in Table 1. Figure 3 provides plots of the first few basis functions obtained from this procedure.

We now describe an algorithm for constructing Fourier representations of Gaussian processes for a range of hyperparameter values.

Algorithm 1. *[Construction of Fourier representations]*

1. Set the interval on which the Gaussian process is defined, $[a, b]$, in addition to the intervals where the hyperparameters $\nu \in [\nu_0, \nu_1]$ and $\rho \in [\rho_0, \rho_1]$ are defined. Additionally, set the error tolerance ϵ for the accuracy of the quadrature, or equivalently accuracy of the effective covariance kernel.
2. Construct a quadrature rule over the region of interest. Specifically, find nodes $\xi_1, \dots, \xi_m \in \mathbb{R}$ and weights $w_1, \dots, w_m \in \mathbb{R}^+$ such that

$$\left| k(d) - \sum_{i=1}^m 2w_i \hat{k}(\xi_i) \cos(\xi_i d) \right| < \epsilon \quad (29)$$

for all $\nu \in [\nu_0, \nu_1]$, $\rho \in [\rho_0, \rho_1]$, and $d \in [0, b - a]$.

3. Define $f : [a, b] \rightarrow \mathbb{R}$ to be the random expansion

$$f(x) \sim \gamma_1 \alpha_1 \cos(\xi_1 x) + \beta_1 \gamma_1 \sin(\xi_1 x) + \dots + \alpha_m \gamma_m \cos(\xi_m x) + \beta_m \gamma_m \sin(\xi_m x) \quad (30)$$

where for $i = 1, \dots, m$ the α_i and β_i are the iid Gaussians

$$\alpha_i, \beta_i \sim \mathcal{N}(0, 1), \quad (31)$$

and where γ_i are defined by

$$\gamma_i = \sqrt{2w_i\hat{k}(\xi_i)} \quad (32)$$

where \hat{k} denotes the Fourier transform of the covariance kernel k and $w_i \in \mathbb{R}$. Then f is a Gaussian process with effective covariance kernel k' defined by

$$k'(d) = \sum_{i=1}^n 2w_i\hat{k}(\xi_j) \cos(\xi_j d). \quad (33)$$

3 Regression

Typically, GP regression is used in the following environment. An applied scientist has observed data $\{(x_i, y_i)_{i=1, \dots, N}\}$ where x_i are independent variables that belong to some interval $[a, b] \in \mathbb{R}$ (for 1-dimensional problems) and $y_i \in \mathbb{R}$ are dependent variables. The observed data y_1, \dots, y_N are assumed to be observations of the form

$$y_i = f(x_i) + \epsilon_i \quad (34)$$

where ϵ_i is iid Gaussian noise and $f : [a, b] \rightarrow \mathbb{R}$ is an unknown function, which is given a Gaussian process prior with covariance function k . Assumptions about k are critical for statistical inference and typically arise from domain expertise or physical knowledge about the data-generating process. There is a large body of literature on the selection of suitable covariance kernels (e.g. [10, 27, 35]). In many applied settings k is not known a priori, but is assumed to belong to some parametric family of functions (e.g. Matérn, squared-exponential, etc.) that depends on hyperparameters that are fit to the data.

The goal of GP regression is to perform statistical inference on the unknown function f at a set of points $\tilde{x} \in [a, b]$ or to understand certain properties of the data-generating process. Inference typically involves evaluating the mean and covariance of the density, conditional on observed data $\mathbf{x}, \mathbf{y} \in \mathbb{R}^N$. The conditional distribution of f at any $\tilde{x} \in \mathbb{R}$ is the Gaussian

$$f(\tilde{x}) | \mathbf{x}, \mathbf{y} \sim \mathcal{N}(\tilde{\mu}, \tilde{\sigma}^2) \quad (35)$$

with

$$\begin{aligned} \tilde{\mu} &= \mathbf{k}(\tilde{x}, \mathbf{x})(\mathbf{K} + \sigma^2 \mathbf{I})^{-1} \mathbf{y} \\ \tilde{\sigma}^2 &= k(\tilde{x}, \tilde{x}) - \mathbf{k}(\tilde{x}, \mathbf{x})(\mathbf{K} + \sigma^2 \mathbf{I})^{-1} \mathbf{k}(\mathbf{x}, \tilde{x}), \end{aligned} \quad (36)$$

where σ is the standard deviation of ϵ_i (also called the nugget), the matrix \mathbf{K} is the $N \times N$ covariance matrix $\mathbf{K}_{i,j} = k(x_i, x_j)$, the vector $\mathbf{k}(\mathbf{x}, x') \in \mathbb{R}^N$ is the column vector such that $\mathbf{k}(\tilde{x}, \mathbf{x})_i = k(\tilde{x}, x_i)$, and $\mathbf{k}(\mathbf{x}, \tilde{x}) = \mathbf{k}(\tilde{x}, \mathbf{x})^\top$.

Since $\mathbf{K} + \sigma^2 \mathbf{I}$ is an $N \times N$ matrix, direct inversion is computationally intractable for large N . However, using the Fourier representations of this paper admits a natural low-rank approximation to \mathbf{K} . Specifically, \mathbf{K} is well-approximated by $\mathbf{X}\mathbf{X}^\top$ where \mathbf{X} is the $N \times 2m$

matrix

$$\mathbf{X} = \begin{bmatrix} \gamma_1 \cos(\xi_1 x_1) & \dots & \gamma_m \cos(\xi_m x_1) & \gamma_1 \sin(\xi_1 x_1) & \dots & \gamma_m \sin(\xi_m x_1) \\ \gamma_1 \cos(\xi_1 x_2) & \dots & \gamma_m \cos(\xi_m x_2) & \gamma_1 \sin(\xi_1 x_2) & \dots & \gamma_m \sin(\xi_m x_2) \\ \vdots & & \vdots & \vdots & & \vdots \\ \gamma_1 \cos(\xi_1 x_N) & \dots & \gamma_m \cos(\xi_m x_N) & \gamma_1 \sin(\xi_1 x_N) & \dots & \gamma_m \sin(\xi_m x_N) \end{bmatrix}. \quad (37)$$

In particular, $\mathbf{K}_{i,j} = k(x_i, x_j)$ and $\mathbf{X}\mathbf{X}^\mathbf{T}$ is the quadrature rule approximation to $k(x_i, x_j)$ given by

$$\sum_{\ell=1}^m 2\hat{k}(\xi_\ell) w_\ell \cos(2\pi \xi_\ell (x_i - x_j)). \quad (38)$$

Using $\mathbf{X}\mathbf{X}^\mathbf{T}$ as the reduced-rank approximation of \mathbf{K} , the linear systems that appear in $\tilde{\mu}$ and $\tilde{\sigma}^2$,

$$(\mathbf{K} + \sigma^2 \mathbf{I})\mathbf{x} = \mathbf{y} \quad \text{and} \quad (\mathbf{K} + \sigma^2 \mathbf{I})\mathbf{x} = \mathbf{k}(\mathbf{x}, \tilde{x}), \quad (39)$$

can be approximated in $O(Nm^2)$ operations using standard direct methods.

For problems where Nm^2 operations is computationally infeasible, the conjugate gradient method (see, e.g., [8]) is an efficient alternative to direct methods, provided $\mathbf{X}\mathbf{X}^\mathbf{T} + \sigma^2 \mathbf{I}$ is well-conditioned. For these problems conjugate gradient has two significant advantages. First, convergence is rapid for well conditioned systems. Specifically, if x is the exact solution to the linear system and \hat{x}_n is the approximate solution after n iterations of conjugate gradient then

$$\|\hat{\mathbf{x}}_n - \mathbf{x}\| = O\left(\left(\frac{\sqrt{\kappa} - 1}{\sqrt{\kappa} + 1}\right)^n\right) \quad (40)$$

where κ is the condition number of the matrix (see e.g. [8]). The second advantage of conjugate gradient in this context is that the matrix $\mathbf{X}\mathbf{X}^\mathbf{T} + \sigma^2 \mathbf{I}$ of the linear system can be applied in $O(N + m^2 \log m)$ time using a type 3 non-uniform FFT [3]. More precisely, the type 3 non-uniform FFT computes, in $O(N + m^2 \log m)$ operations, the sums f_ℓ defined by

$$f_\ell = \sum_{j=1}^N c_j e^{i\xi_\ell x_j} \quad (41)$$

for $\ell = 1, \dots, m$ for any $c_1, \dots, c_N \in \mathbb{C}$, $\xi_1, \dots, \xi_m \in \mathbb{R}$ and $x_1, \dots, x_N \in \mathbb{R}$. Contrary to the standard FFT, in the non-uniform FFT the ξ_i and x_i need not be uniformly spaced.

3.1 Weight-space inference

In the weight-space approach to inference, the posterior density is defined over the coefficients of the basis function expansion – in this paper a Fourier expansion. Specifically, given data $\{(x_i, y_i)\}$ and a covariance kernel k , Gaussian process regression becomes

$$\begin{aligned} \mathbf{y} &\sim \mathbf{X}\boldsymbol{\beta} + \boldsymbol{\epsilon} \\ \boldsymbol{\epsilon} &\sim \mathcal{N}(0, \sigma^2 \mathbf{I}) \\ \boldsymbol{\beta} &\sim \mathcal{N}(0, \mathbf{I}) \end{aligned} \quad (42)$$

where $\boldsymbol{\beta} \in \mathbb{R}^{2m}$ is the vector of coefficients and \mathbf{X} is the $N \times 2m$ matrix (37). The posterior density corresponding to (42) is defined over $2m$ dimensions, the components of $\boldsymbol{\beta}$ (or $2m+1$ including the residual standard deviation σ). The conditional distribution of $\boldsymbol{\beta}$ (conditioning on $\sigma, \mathbf{x}, \mathbf{y}$) is Gaussian. Specifically,

$$\boldsymbol{\beta} | \sigma, \mathbf{x}, \mathbf{y} \sim \mathcal{N}(\bar{\boldsymbol{\beta}}, (\mathbf{X}^\top \mathbf{X} + \sigma^2 \mathbf{I})^{-1}) \quad (43)$$

where $\bar{\boldsymbol{\beta}}$ is the solution to the linear system of equations

$$(\mathbf{X}^\top \mathbf{X} + \sigma^2 \mathbf{I})\bar{\boldsymbol{\beta}} = \mathbf{X}^\top \mathbf{y}. \quad (44)$$

The conditional mean $\bar{\boldsymbol{\beta}} \in \mathbb{R}^{2m}$ is the vector of coefficients of the conditional mean function

$$\sum_{i=1}^m \bar{\beta}_{1,i} \cos(\xi_i x) + \bar{\beta}_{2,i} \sin(\xi_i x) \quad (45)$$

for all $x \in [a, b]$.

We now describe a numerical implementation of a solver for this system of equations that requires $O(N + m^3)$ operations by taking advantage of the Fourier representation of GPs.

3.2 Numerical Implementation

For a general $N \times 2m$ matrix \mathbf{X} , the computational complexity of the numerical solution of the linear system of equations

$$(\mathbf{X}^\top \mathbf{X} + \sigma^2 \mathbf{I})\mathbf{x} = \mathbf{X}^\top \mathbf{y} \quad (46)$$

is $O(Nm^2)$. For GP regression tasks with large amounts of data, $O(Nm^2)$ can be prohibitively expensive. However for the linear system that appears in the case of Fourier representations, we take advantage of the structure of \mathbf{X} to reduce evaluation to $O(N + m^3)$ operations. We do this by constructing the $2m \times 2m$ matrix $\mathbf{X}^\top \mathbf{X}$ in $O(N + m^2 \log m)$ operations using a non-uniform fast Fourier transform (FFT) [9, 17] whereas constructing $\mathbf{X}^\top \mathbf{X}$ ordinarily requires $O(Nm^2)$ operations for general matrices.

The $N \times 2m$ matrix \mathbf{X} has the form

$$\mathbf{X} = \begin{bmatrix} \gamma_1 \cos(\xi_1 x_1) & \dots & \gamma_m \cos(\xi_m x_1) & \gamma_1 \sin(\xi_1 x_1) & \dots & \gamma_m \sin(\xi_m x_1) \\ \gamma_1 \cos(\xi_1 x_2) & \dots & \gamma_m \cos(\xi_m x_2) & \gamma_1 \sin(\xi_1 x_2) & \dots & \gamma_m \sin(\xi_m x_2) \\ \vdots & & \vdots & \vdots & & \vdots \\ \gamma_1 \cos(\xi_1 x_N) & \dots & \gamma_m \cos(\xi_m x_N) & \gamma_1 \sin(\xi_1 x_N) & \dots & \gamma_m \sin(\xi_m x_N) \end{bmatrix}.$$

where γ_i is defined by

$$\gamma_i = \sqrt{2\hat{k}(\xi_i)w_i}. \quad (47)$$

for $i = 1, \dots, m$ where \hat{k} is the Fourier transform of the covariance function, and $w_i, \xi_i > 0$ are the nodes and weights of (29). We observe that $\mathbf{X}^\top \mathbf{X}$ can be factorized as

$$\mathbf{X}^\top \mathbf{X} = \mathbf{B}^\top \mathbf{D} \mathbf{X}'^\top \mathbf{X}' \mathbf{D} \mathbf{B} \quad (48)$$

where \mathbf{X}' is defined by

$$\mathbf{X}' = \begin{bmatrix} e^{i\xi_1 x_1} & \dots & e^{i\xi_m x_1} & e^{i(-\xi_1)x_1} & \dots & e^{i(-\xi_m)x_1} \\ e^{i\xi_1 x_2} & \dots & e^{i\xi_m x_2} & e^{i(-\xi_1)x_2} & \dots & e^{i(-\xi_m)x_2} \\ \vdots & & \vdots & \vdots & & \vdots \\ e^{i\xi_1 x_N} & \dots & e^{i\xi_m x_N} & e^{i(-\xi_1)x_N} & \dots & e^{i(-\xi_m)x_N} \end{bmatrix}, \quad (49)$$

where \mathbf{D} is the diagonal $2m \times 2m$ matrix

$$\mathbf{D} = \begin{bmatrix} \gamma_1 & & & & & \\ & \ddots & & & & \\ & & \gamma_m & & & \\ & & & \gamma_1 & & \\ & & & & \ddots & \\ & & & & & \gamma_m \end{bmatrix}, \quad (50)$$

and \mathbf{B} is $2m \times 2m$ block matrix

$$\mathbf{B} = \begin{bmatrix} \frac{1}{2} \mathbf{I}_m & \frac{1}{2i} \mathbf{I}_m \\ \frac{1}{2} \mathbf{I}_m & -\frac{1}{2i} \mathbf{I}_m \end{bmatrix} \quad (51)$$

where \mathbf{I}_m denotes the $m \times m$ identity matrix. The matrix $\mathbf{X}'^\top \mathbf{X}'$ is a symmetric matrix where entry i, ℓ is given by

$$(\mathbf{X}'^\top \mathbf{X}')_{i,\ell} = \sum_{j=1}^N e^{ix_j(\xi_i + \xi_\ell)}, \quad (52)$$

for all $i, \ell \in \{1, \dots, 2m\}$, where we denote $-\xi_i$ with ξ_{m+i} . The sums of (52) can be evaluated with a type 3 non-uniform FFT, a calculation that requires $O(N + m^2 \log m)$ operations. More precisely, we use the type 3 non-uniform FFT of [3] to compute the sums

$$\sum_{j=1}^N e^{ix_j \omega_\ell} \quad (53)$$

where $\ell = 1, \dots, 2m^2 + m$ and $\omega_\ell = \xi_p + \xi_q$ for $p, q \in \{1, \dots, 2m\}$ with $q \geq p$. We also use the non-uniform FFT to compute $\mathbf{X}^\top \mathbf{y}$, the right hand side of (46).

Since matrix multiplications of (48) other than $\mathbf{X}'^\top \mathbf{X}'$ can be applied in $O(m^2)$ operations, the total complexity of forming matrix $\mathbf{X}^\top \mathbf{X}$ using a non-uniform FFT is $O(N + m^2 \log m)$. Once $\mathbf{X}^\top \mathbf{X}$ is formed, the resulting linear system can be solved in $O(m^3)$ operations using standard direct methods. In the following, we provide an algorithm for solving linear system (46) in $O(N + m^3)$ operations.

Algorithm 2. *[GP regression solver]*

1. Use Algorithm 1 to construct nodes ξ_1, \dots, ξ_m and weights w_1, \dots, w_m of a Fourier expansion for a certain covariance kernel or family of kernels.
2. Use the non-uniform FFT to compute the matrix-vector product

$$\mathbf{X}^\top \mathbf{y} \quad (54)$$

that appears in the right hand side of (46).

3. Use the non-uniform FFT to compute the sums

$$\sum_{j=1}^N e^{ix_j \omega_\ell} \quad (55)$$

where $\ell = 1, \dots, 2m^2 + m$ and $\omega_\ell = \xi_p + \xi_q$ for $p, q \in \{1, \dots, 2m\}$ with $q \geq p$.

4. Construct $\mathbf{X}^\top \mathbf{X}$ via

$$\mathbf{X}^\top \mathbf{X} = \mathbf{B}^\top \mathbf{D} \mathbf{X}'^\top \mathbf{X}' \mathbf{D} \mathbf{B} \quad (56)$$

where \mathbf{D} is defined in (50) and \mathbf{B} is defined in (51).

5. Compute the eigendecomposition of $\mathbf{X}^\top \mathbf{X}$. That is, find the $2m \times 2m$ orthogonal matrix \mathbf{U} and the diagonal $2m \times 2m$ matrix \mathbf{S} such that

$$\mathbf{X}^\top \mathbf{X} = \mathbf{U} \mathbf{S} \mathbf{U}^\top \quad (57)$$

6. Compute the solution to linear system (46) via

$$\mathbf{x} = \mathbf{U}(\mathbf{S} + \sigma^2 \mathbf{I})^{-1} \mathbf{U}^\top \mathbf{X}^\top \mathbf{y}. \quad (58)$$

In Table 3 we provide computation times for solving the linear system of equations (46) as well as forming $\mathbf{X}^\top \mathbf{X}$ and the matrix vector multiply $\mathbf{X}^\top \mathbf{y}$. Additionally, in Figure 2 we plot the total computation times for GP regression for various amounts of data.

3.3 Adaptation of hyperparameters

In certain GP problems, the covariance function, k is known a priori, however in most environments, k is assumed to belong to a certain parametric family of functions (e.g. Matérn, squared-exponential, etc.) that depends on hyperparameters that are fit to the data. Methods for fitting hyperparameters to data involve performing GP regression and solving the linear system of equations (46) for many hyperparameter values.

For those problems, the methods of this paper have several advantages:

- Algorithm 1 can be used to generate a Fourier expansion that is valid over the posterior domain of hyperparameters. That expansion depends on hyperparameters by a rescaling of basis functions (or equivalently by rescaling the standard deviation of the coefficients).

- Using Algorithm 2, GP regression is performed in $O(m^3)$ operations for all hyperparameters after a precomputation of $O(N + m^2 \log m)$ operations. The precomputation involves the applications of non-uniform FFTs (steps 2 and 3 of Algorithm 2).
- Since both the observation noise and the priors on regression coefficients are Gaussian, the posterior density in the coefficients β is also Gaussian. As a result, efficient numerical methods can be used for evaluating Bayesian posterior moments [16, 23], in particular the algorithm of [17] for fitting hyperparameters of GP models.
- Evaluation of gradients for maximum likelihood estimates can be performed in $O(m^2)$ operations after inversion of the posterior covariance matrix (step 5 in Algorithm 2). The component-wise formula for the gradient of the log-likelihood of the posterior density is given by

$$\frac{\partial}{\partial \theta_j} \log(p(\mathbf{y}|\boldsymbol{\theta})) = \frac{1}{2} \mathbf{y}^\top \mathbf{C}^{-1} \frac{\partial \mathbf{C}}{\partial \theta_j} \mathbf{C}^{-1} \mathbf{y} - \frac{1}{2} \text{tr} \left(\mathbf{C}^{-1} \frac{\partial \mathbf{C}}{\partial \theta_j} \right) \quad (59)$$

where $\theta_j \in \mathbb{R}$ is the j -th hyperparameter (see e.g. [31]), and $\mathbf{C} = (\mathbf{X}^\top \mathbf{X} + \sigma^2 \mathbf{I})$.

4 Numerical Experiments

In this section we demonstrate the performance of the algorithms of this paper on randomly generated data. We implemented Algorithm 1 and Algorithm 2 in Fortran with the GFortran compiler on a 2.6 GHz 6-Core Intel Core i7 MacBook Pro. All examples were run in double precision arithmetic.

We used Algorithm 1 to construct Fourier expansions for the Gaussian processes defined on $[-1, 1]$ with Matérn kernel, $k_{\nu, \rho}$ defined by

$$k(r) = \frac{2^{1-\nu}}{\Gamma(\nu)} \left(\sqrt{2\nu} \frac{r}{\rho} \right)^\nu K_\nu \left(\sqrt{2\nu} \frac{r}{\rho} \right) \quad (60)$$

for all $\nu \in [3/2, 7/2]$ and $\rho \in [0.1, 0.5]$. We used the implementation of [32] for the generalized Gaussian quadrature with $\epsilon = 10^{-5}$ in Algorithm 1. The total run time for generating the quadrature was 88 seconds. The output of the code was 86 total nodes and weights and all weights were positive.

Figure 1 is a plot of the locations of the nodes obtained from this procedure. In Table 1 we list those nodes and the corresponding weights.

In Table 2 we provide the L^2 error of the effective covariance kernel for various values of ν and ρ . The L^2 error of the effective kernel is defined by the formula

$$\left(\int_{-1}^1 \int_{-1}^1 (k'(x, y) - k(x, y))^2 dx dy \right)^{1/2} \quad (61)$$

where k' denotes the effective covariance kernel and k denotes the true kernel. Integral (61) was computed numerically using a tensor product of Gaussian nodes and weights.

Table 3 contains the results of numerical experiments for Gaussian process regression using Algorithms 1 and 2. The data, $\{(x_i, y_i)\}$ was randomly generated on the interval $[-1, 1]$ via

$$y_i = \cos(3e^{x_i}) + \epsilon_i \quad (62)$$

where

$$\epsilon_i \sim \mathcal{N}(0, 0.5). \quad (63)$$

The x_i are equispaced on $[-1, 1]$. The nodes and weights of the Fourier expansions used are given by Table 2. We used Algorithm 2 to compute the conditional mean and covariance and report timings in Table 3 where N denotes the number of data points, ν, ρ denote the hyperparameters of the Matérn kernel, and the column “ σ^2 ” denotes the residual variance (or nugget). The L^2 error of the effective covariance kernel (see (61)) is provided in the column “ L^2 error”. We include timings for solving the regression problem via Algorithm 2. In column “FFT time (s)” we provide the total time for formation of the matrix $\mathbf{X}^\top \mathbf{X}$ and the matrix vector multiply $\mathbf{X}^\top \mathbf{y}$. The column “solve time (s)” denotes the remaining time in the regression solution, which involves inversion of $(\mathbf{X}^\top \mathbf{X} + \sigma^2 \mathbf{I})$.

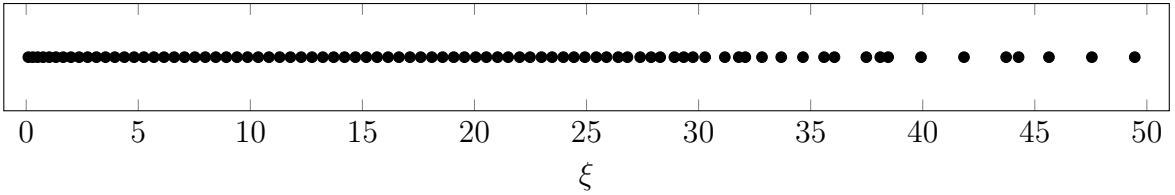


Figure 1: *Location of the 86 nodes for GPs defined on $[-1, 1]$ with Matérn kernels with $\nu \in [1.5, 3.5]$, and $\rho \in [0.1, 0.5]$.*

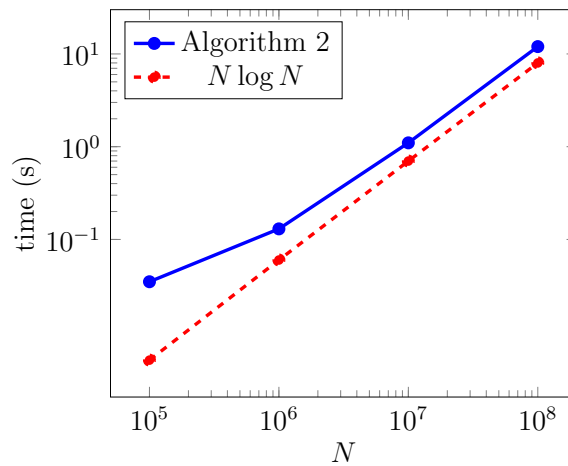


Figure 2: Scaling times for evaluation of conditional mean for varying amounts of data. We include a plot proportional to $N \log N$ for comparison.

i	nodes	weights	i	nodes	weights
1	0.0960748783232733	0.1933002284075283	44	18.5783668916359304	0.4901095181946152
2	0.2949311558758212	0.2064005047360611	45	19.0739289334232396	0.4936700008508603
3	0.5121811831688609	0.2293690006634405	46	19.5535187961381212	0.4806551264127251
4	0.7553750530381257	0.2574584689846101	47	20.0540157049340202	0.4919980518793062
5	1.0272554775524241	0.2860863008101612	48	20.5303087220011804	0.4886725084331118
6	1.3267469591800769	0.3123806483750251	49	21.0308285956013101	0.4985884540483315
7	1.6509109783729810	0.3353906370922179	50	21.5033438976054896	0.4525339724563319
8	1.9964656597608781	0.3552203181130367	51	22.0147025165826093	0.5300911113825829
9	2.3604331716760738	0.3722929241325456	52	22.4786227659423616	0.4703295964417554
10	2.7402749478447399	0.3870336516793261	53	22.9890428278831500	0.5031381396430530
11	3.1338448880682450	0.3998022537083804	54	23.4620311240316504	0.4385610519729455
12	3.5393213277133500	0.4108896687408796	55	23.9659051179655798	0.5529348248583776
13	3.9551382871240710	0.4205230182176792	56	24.4374955606510014	0.4879736648158969
14	4.3799500415428971	0.4289035535544789	57	24.9268582817982995	0.4320150910275336
15	4.8125843418627330	0.4361897874230700	58	25.4355862458376691	0.5030088994396542
16	5.2520252807076444	0.4425587482527165	59	25.8908822711706499	0.4986129817647325
17	5.6973962780821781	0.4480785412063698	60	26.4135765170375585	0.5698981287926346
18	6.1479398698978196	0.4528922343761104	61	26.8244665781450813	0.3580010222446956
19	6.6029703189280022	0.4571127652712647	62	27.3929596371526216	0.4477770521368305
20	7.0619657471053916	0.4607536593597344	63	27.8810764015625807	0.6306236380217451
21	7.5244050646589304	0.4640030341808996	64	28.2872085273741511	0.5684848926018280
22	7.9898781249339503	0.4668744890692324	65	28.9186103516193818	0.1661641302432533
23	8.4580188390522402	0.4693377032983527	66	29.3361902609053793	0.7145700506865926
24	8.9284697412154603	0.4715695985713800	67	29.7475402852299098	0.3653264402765759
25	9.4010606000280621	0.4735626358176499	68	30.2919596593750207	0.7987670620900847
26	9.8755021184860947	0.4753261760015748	69	31.1707837877708087	0.6496969625503436
27	10.3515866576509996	0.4768203234940871	70	31.7921709344750916	0.6374198048803309
28	10.8290813405759305	0.4782250403991462	71	32.0844373549515112	0.4525776393523478
29	11.3078856905533307	0.4795013762603529	72	32.8290834819148998	0.5792967675329964
30	11.7878547186769005	0.4806019700535451	73	33.6870452221527970	1.2316989151794200
31	12.2690444362196605	0.4816049378992831	74	34.6556177080743311	0.6653181217090052
32	12.7507923286660407	0.4826033499503408	75	35.5973697159031417	0.7979748203948971
33	13.2340308273640499	0.4830779751411056	76	36.0608079398967192	0.9871538295211217
34	13.7168180215943405	0.4845298908539934	77	37.4828497993489194	1.1429690155529550
35	14.2023546685620694	0.4833485049199899	78	38.1056387575873927	0.3983778654241495
36	14.6852339737999902	0.4872979567198063	79	38.4560335475650206	0.7492963615598504
37	15.1736671929864606	0.4828723127156595	80	39.9230354160448471	1.7911442981045280
38	15.6561205601530808	0.4883987918117061	81	41.8408663755605872	1.9661520413352620
39	16.1465532564475396	0.4852092322682524	82	43.7213283268615385	1.6715931870761731
40	16.6287678133340897	0.4863731168868852	83	44.2767860363890975	0.2685526601061519
41	17.1217168205720291	0.4871456130687457	84	45.6320859437675992	1.7725506245674350
42	17.6027784484422583	0.4894715943022971	85	47.5466594857420191	1.9715488370126710
43	18.0975219052295202	0.4843933188273860	86	49.4591701554423580	1.5256479816263220

Table 1: *Nodes and weights for GPs defined on $[-1, 1]$ with Matérn kernels with $\nu \in [0.5, 3.5]$, and $\rho \in [0.1, 0.5]$*

5 Generalizations and Conclusions

In this paper we introduce algorithms for representing and computing with Gaussian processes in 1-dimension. In Algorithm 1, we describe a numerical scheme for representing families of Gaussian processes as Fourier expansions of the form

$$f(x) \sim \gamma_1 \alpha_1 \cos(\xi_1 x) + \beta_1 \gamma_1 \sin(\xi_1 x) + \dots + \alpha_m \gamma_m \cos(\xi_m x) + \beta_m \gamma_m \sin(\xi_m x) \quad (64)$$

where for $i = 1, \dots, m$ the coefficients $\xi_i \in \mathbb{R}$ are fixed, and α_i and β_i are the iid Gaussians

$$\alpha_i, \beta_i \sim \mathcal{N}(0, 1), \quad (65)$$

ν	ρ	L^2 error
1.5	0.1	0.780×10^{-4}
1.5	0.3	0.295×10^{-5}
1.5	0.5	0.140×10^{-5}
2.0	0.1	0.141×10^{-4}
2.0	0.3	0.611×10^{-6}
2.0	0.5	0.118×10^{-4}
2.5	0.1	0.326×10^{-5}
2.5	0.3	0.608×10^{-6}
2.5	0.5	0.445×10^{-6}
3.0	0.1	0.113×10^{-5}
3.0	0.3	0.577×10^{-6}
3.0	0.5	0.239×10^{-6}
3.5	0.1	0.693×10^{-6}
3.5	0.3	0.630×10^{-6}
3.5	0.5	0.222×10^{-6}

Table 2: *Accuracy of Fourier expansion with nodes and weights of Table 1 for Matérn kernels with various hyperparameter values.*

N	ν	ρ	σ^2	L^2 error	FFT time (s)	solve time (s)	total time (s)
10^5	3.0	0.1	0.5	0.113×10^{-5}	0.03	0.004	0.035
10^6	2.0	0.5	0.6	0.118×10^{-4}	0.11	0.005	0.12
10^7	1.5	0.1	3.0	0.780×10^{-4}	1.1	0.004	1.1
10^8	3.5	0.3	0.95	0.630×10^{-6}	12.0	0.005	12.0

Table 3: *Computation times and accuracy of effective kernel for GP regression nodes and weights of Table 1. The GP is defined on $[-1, 1]$ with Matérn kernels with $\nu \in [0.5, 3.5]$, and $\rho \in [0.1, 0.5]$.*

and where γ_i , are defined by

$$\gamma_i = \sqrt{2w_i \hat{k}(\xi_i)} \quad (66)$$

where \hat{k} denotes the Fourier transform of the covariance kernel k and $w_i \in \mathbb{R}$. where α_i and β_i are iid standard normal random variables. These expansions are constructed in such a way that they are valid over families of covariance kernels. Representing a GP as expansion (64), allows the use Algorithm 2 to perform GP regression in $O(N + m^3)$ time where N is the number of data points and m the size of the expansion.

While this paper is focused on GPs in 1-dimensions, much of the theory and numerical machinery extends naturally to higher dimensions. In particular, for GPs over \mathbb{R}^d , one generalization of the 1-dimensional Fourier expansion is the tensor-product expansion of the form

$$f(\mathbf{x}) \sim \sum_{\mathbf{j} \in \{1, \dots, m\}^d} \alpha_{\mathbf{j}} e^{i2\pi \langle \boldsymbol{\xi}_{\mathbf{j}}, \mathbf{x} \rangle} \quad (67)$$

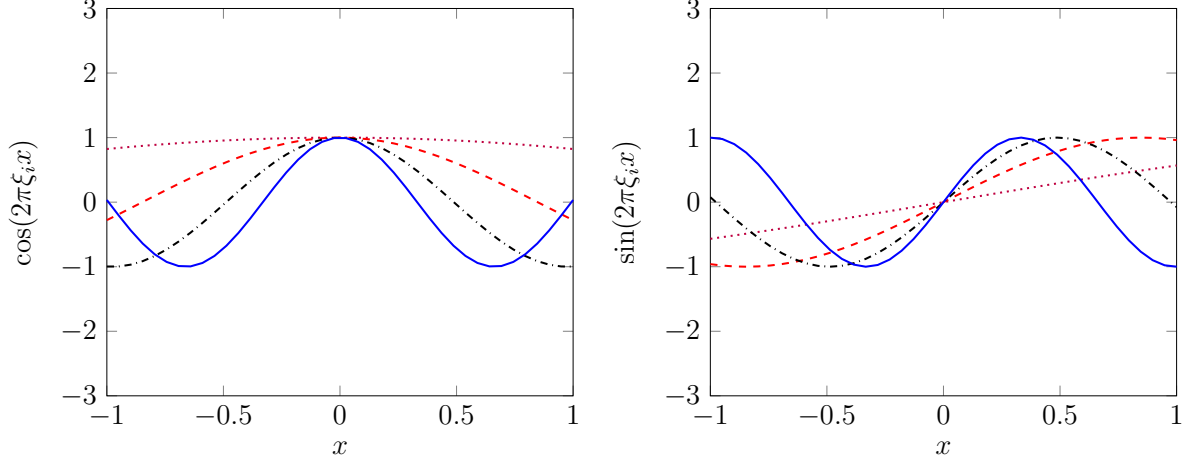


Figure 3: The first 4 basis functions $\cos(2\pi\xi_i x)$ and $\sin(2\pi\xi_i x)$ for the Matérn kernel with $\nu \in [1.5, 3.5]$, $\rho \in [0.1, 0.5]$, and nodes and weights of Table 1.

where $\mathbf{x} \in \mathbb{R}^d$, $\boldsymbol{\xi}_{\mathbf{j}} = (\xi_{j_1}, \xi_{j_2}, \dots, \xi_{j_d})$ where ξ_1, \dots, ξ_m are real-valued frequencies. As in the 1-dimensional case, the weight-space linear system of equations in the d -dimensional GP regression contains structure that's amenable to fast algorithms. For example, the matrix of the weight-space linear system can be applied efficiently using the non-uniform fast Fourier transform.

We plan to address the higher dimensional extension of the tools of this paper in subsequent publications.

References

- [1] S. Ambikasaran, D. Foreman-Mackey, L. Greengard, D. W. Hogg, and M. O’Neil. Fast Direct Methods for Gaussian Processes. *IEEE Trans. Pattern Anal. Mach. Intell.*, 38(2):252–265, 2016.
- [2] S. Banerjee, A. E. Gelfand, A. O. Finley, and H. Sang. Gaussian predictive process models for large spatial data sets. *Royal Statistical Society*, 70(4):825–848, 2008.
- [3] A. H. Barnett, J. Magland, and L. af Klinteberg. A parallel nonuniform fast fourier transform library based on an “exponential of semicircle” kernel. *SIAM Journal on Scientific Computing*, 41(5):C479–C504, 2019.
- [4] A. P. Bartók, M. C. Payne, R. Kondor, and G. Csányi. Gaussian approximation potentials: The accuracy of quantum mechanics, without the electrons. *Phys. Rev. Lett.*, 104:136403, Apr 2010.
- [5] J. Bremer and Z. Gimbutas. A nyström method for weakly singular integral operators on surfaces. *Journal of Computational Physics*, 231(14):4885–4903, 2012.
- [6] J. Bremer, Z. Gimbutas, and V. Rokhlin. A nonlinear optimization procedure for generalized gaussian quadratures. *SIAM Journal on Scientific Computing*, 32(4):1761–1788, 2010.
- [7] N. Cressie. *Statistics for Spatial Data, Revised Edition*. Wiley-Interscience, Hoboken, NJ, 2015.
- [8] G. Dahlquist and A. Bjork. *Numerical Methods*. Dover, Mineola, NY, 1974.
- [9] A. Dutt and V. Rokhlin. Fast fourier transforms for nonequispaced data. *SIAM Journal on Scientific Computing*, 14(6):1368–1393, 1993.
- [10] D. Duvenaud. *Automatic Model Construction with Gaussian Processes*. PhD thesis, Computational and Biological Learning Laboratory, University of Cambridge, 2014.
- [11] S. Filip, A. Javeed, and L. N. Trefethen. Smooth Random Functions, Random ODEs, and Gaussian Processes. *SIAM Review*, 61(1):185–205, 2019.
- [12] D. Foreman-Mackey, E. Agol, S. Ambikasaran, and R. Angus. Fast and Scalable Gaussian Process Modeling with Applications to Astronomical Time Series. *The Astronomical Journal*, 154(6), 2017.
- [13] A. Gelman, J. B. Carlin, H. S. Stern, D. B. Dunson, A. Vehtari, and D. B. Rubin. *Bayesian Data Analysis*. Chapman and Hall/CRC, New York, NY, 3rd edition, 2013.
- [14] J. Gonzalez, E. Lezmi, T. Roncalli, and J. Xu. Financial Applications of Gaussian Processes and Bayesian Optimization. *arXiv*, q-fin/1903.04841, 2019.
- [15] L. Greengard and J.-Y. Lee. Accelerating the nonuniform fast fourier transform. *SIAM Review*, 46(3):443–454, 2004.

- [16] P. Greengard, A. Gelman, and A. Vehtari. A Fast Regression via SVD and Marginalization. *Computational Statistics*, 2021.
- [17] P. Greengard and M. O’Neil. Efficient reduced-rank methods for gaussian processes with eigenfunction expansions. *arXiv*, stat.CO/2108.05924, 2021.
- [18] J. Hensman, N. Durrande, and A. Solin. Variational fourier features for gaussian processes. *J. Mach. Learn. Res.*, 18(1):5537–5588, 2017.
- [19] J. G. Hoskins, V. Rokhlin, and K. Serkh. On the numerical solution of elliptic partial differential equations on polygonal domains. *SIAM Journal on Scientific Computing*, 41(4):A2552–A2578, 2019.
- [20] S. Karlin and W. Studden. *Tchebycheff Systems with Applications in Analysis and Statistics*. Wiley-Interscience, 1966.
- [21] M. Lázaro-Gredilla, J. Quiñero-Candela, C. E. Rasmussen, and A. R. Figueiras-Vidal. Sparse spectrum gaussian process regression. *Journal of Machine Learning Research*, 11(63):1865–1881, 2010.
- [22] M. Lázaro-Gredilla, J. Quiñero-Candela, C. E. Rasmussen, and A. R. Figueiras-Vidal. Sparse spectrum gaussian process regression. *Journal of Machine Learning Research*, 11(63):1865–1881, 2010.
- [23] D. V. Lindley and A. F. M. Smith. Bayes estimates for the linear model. *Journal of the Royal Statistical Society. Series B (Methodological)*, 34(1):1–41, 1972.
- [24] R. Luger, D. Foreman-Mackey, and C. Hedges. Mapping stellar surfaces. ii. an interpretable gaussian process model for light curves. *The Astronomical Journal*, 162:124, Aug 2021.
- [25] J. Ma, V. Rokhlin, and S. Wandzura. Generalized gaussian quadrature rules for systems of arbitrary functions. *SIAM Journal on Numerical Analysis*, 33(3):971–996, 1996.
- [26] V. Minden, A. Damle, K. L. Ho, and L. Ying. Fast Spatial Gaussian Process Maximum Likelihood Estimation via Skeletonization Factorizations. *Multiscale Modeling and Simulation*, 15(4), 2017.
- [27] T. Paananen, J. Piironen, M. R. Andersen, and A. Vehtari. Variable selection for gaussian processes via sensitivity analysis of the posterior predictive distribution. In *Proceedings of the Twenty-Second International Conference on Artificial Intelligence and Statistics*, volume 89, pages 1743–1752. PMLR, 16–18 Apr 2019.
- [28] J. Quiñero-Candela and C. E. Rasmussen. Analysis of some methods for reduced rank Gaussian process regression. In *Switching and learning in feedback systems*, pages 98–127. Springer, 2005.
- [29] A. Rahimi and B. Recht. Random features for large-scale kernel machines. In J. Platt, D. Koller, Y. Singer, and S. Roweis, editors, *Advances in Neural Information Processing Systems*, volume 20. Curran Associates, Inc., 2008.

- [30] A. Rahimi and B. Recht. Random features for large-scale kernel machines. In J. Platt, D. Koller, Y. Singer, and S. Roweis, editors, *Advances in Neural Information Processing Systems*, volume 20. Curran Associates, Inc., 2008.
- [31] C. E. Rasmussen and C. L. I. Williams. *Gaussian Processes for Machine Learning*. MIT Press, Cambridge, MA, 2006.
- [32] K. Serkh. *Personal correspondence*, 2021.
- [33] P. F. Shustin and H. Avron. Gauss-legendre features for gaussian process regression, 2021.
- [34] A. Solin and S. Särkkä. Hilbert space methods for reduced-rank Gaussian process regression. *Statistics and Computing*, 30, 2020.
- [35] M. L. Stein. *Interpolation of Spatial Data, Some Theory for Kriging*. Springer, New York, NY, 1999.
- [36] L. N. Trefethen. *Approximation Theory and Approximation Practice: Extended Edition*. SIAM, Philadelphia, PA, 2020.